

# White Light Spectroscopy for Mammalian Cell Viability/Quality Assessment: Towards an Online, Label-Free and Sampling-Less System to Simplify Quality Control in CAR T-Cells Production

Bruno Wacogne<sup>1,2</sup>, Céline Codjiova<sup>1</sup>, Jovanne Palvair<sup>1</sup>, Naïs Vaccari<sup>1</sup>, Mélanie Couturier<sup>3</sup>,  
Alain Rouleau<sup>1</sup> and Annie Frelet-Barrand<sup>1</sup>

<sup>1</sup>Université de Franche-Comté, CNRS, institut FEMTO-ST, F-25000 Besançon, France

<sup>2</sup>Centre Hospitalier Universitaire de Besançon, Centre d'Investigation Clinique, INSERM CIC 1431,  
25000, Besançon, France

<sup>3</sup>MedInnPharma, 4 rue Charles Bried, 25000 Besançon France

**Keywords:** White Light Spectroscopy, Mammalian Cells, Viability, Car T-Cells.

**Abstract:** CAR T-cells are highly promising medical products for personalized medicine, but their long production is complex and require extensive quality controls, which result in prohibitive costs for most patients. These controls include monitoring of cell concentration, viability, and possible contamination detection. To simplify CAR T production, these controls should ideally be conducted online in a closed system, without sampling from the bioreactor. Recently, we proposed white light spectroscopy as a method for online monitoring of cell concentration. In this paper, we demonstrate that this optical method can also assess cell viability. We define a cell suspension "quality value" which shows a linear relationship with cell viability estimated by conventional methods. This relationship varies depending on the techniques used and the dominant T-cell death process induced. We then hypothesise that the quality score could serve as a general indicator of cell suspension health, as it is not dependent on any biophysical-chemical interaction or instrument. Overall, the correlation between conventional and optical methods, together with previously published results on cell concentration monitoring, suggests that white light spectroscopy is a promising on-line and sample-free option for monitoring CAR T production.

## 1 INTRODUCTION

CAR T-cells are promising advanced therapy drugs. Their manufacturing process is quite complex (Wang, 2016; Wang, 2023) and quality control is daily performed at each step and especially during the expansion phase. Quality control reside mostly in monitoring cell concentrations, assessing cell viability, and detecting potential contamination. We have recently proposed a proof of concept for a potentially sampling-less white light spectroscopy system for monitoring T-cell concentrations (Wacogne 2020, 2021, 2022). The goal of our current work is to explore the potential of white light spectroscopy for assessing cell viability. Indeed, cell viability measurement is a critical technique in biological research, drug development, and clinical applications used to assess cell health, proliferation,

and survival under various experimental conditions. However, cell viability assessment remains a challenge for label-free and online applications. A wide range of methods have been developed to quantify/measure cell viability, based on specific cell type, experimental objectives, and available resources.

### *Traditional Techniques*

The trypan blue dye exclusion assay is the historical technique of assessing cell viability (Macklin, 1920). It distinguishes live cells from dead ones based on membrane integrity. Viable cells exclude the dye, while dead cells retain it (Louis, 2011). In some cases, trypan blue may also have an effect on cell morphology and viability depending on dye concentration (Tsaouis, 2013). Cell sampling is required as cells must be collected from the culture,

mixed with the dye, and then manually counted using a hemocytometer or automated cell counter. Although cost-effective, its low sensitivity and manual counting introduce limitations, particularly for high-throughput or highly accurate experiments (Stoddart, 2011). However, the use of  $\text{Ni}^{2+}$  or  $\text{Co}^{2+}$  salts may help improving the assay sensitivity (Sarma, 2000).

Other techniques could be used. The MTT and MTS assays measure mitochondrial reduction of tetrazolium salts into formazan by viable cells. Cells do not need to be sampled from the culture for immediate analysis but, at the end of the assay, the cell medium is sampled to measure the color change associated with formazan production using a spectrophotometer. This method, though easy to perform, depends on mitochondrial activity, which can vary with cell type and condition (Berridge, 2016). In the case of irradiated HepG2 cells (Chung, 2015), a decrease of cell viability was observed using trypan blue while no significant changes could be detected using MTT assay. This indicates that the viability detection principle should be adapted to the cell death process.

LDH assays can also quantify cell death by measuring LDH released by damaged cells into the medium (Zou, 2013). Sampling of cell supernatant is required to analyse extracellular LDH levels, typically performed after an incubation period to allow sufficient LDH release. While this method is sensitive to early cell death, it cannot distinguish between apoptosis and necrosis. LDH and MTT assays were compared to study cytotoxicity of cadmium chloride on HTC and HepG2 cells (Fotakis, 2006) and MTT assay exhibit a higher sensitivity compared to LDH assay.

#### *Advanced Techniques*

Other methods have been developed. Among them, flow cytometry enables precise identification of live, apoptotic and dead cells by using reagents such as fluorescent dyes, cell impermeant viability dyes or leukocyte markers for example. Sampling of cell suspension is required to collect and stain cells before analysis through cytometer. This technique is a gold standard for high-throughput applications due to its precision in cell viability measurement (Shenkin, 2007) and allows detecting both apoptosis and necrosis (Kumar, 2015).

Fluorescence microscopy assays use different dyes to stain live cells (for example, AlamarBlue; Hamalainen-Laanaya, 2012). Dyes are added to cell culture, and after incubation, images are captured to quantify cell viability. The accuracy of automated image analysis and high-content screening provides

quantitative results, especially for high-throughput studies. However, exposure to excitation light may alter cell viability itself and tolerable light doses must be employed (Schneckenburger, 2012). It was found that the cell morphologic changes due to trypan blue makes them difficult to count under microscope generating an artificially higher viability compared to fluorescence methods and could result in viability measurement differences between these methods (Chan, 2015).

Impedance-based methods can track cell viability by measuring electrical impedance as cells attach and spread on electrode-coated plates. It is label-free, non-invasive and monitors cell continuously and in real time, offering high sensitivity and accuracy without disrupting the cells and does not require sampling of cell solution. However, cells must spread on coated plates or micromachined substrates which makes it difficult to implement in conventional laboratories (Optiz, 2019; Zhong, 2021; Yang, 2023).

Microfluidic devices enable high-throughput and low-volume viability assays at single-cell level. Sampling is not typically required as the fluidics system controls cell and reagents introduction and analysis is performed within microchannels. Cell viability assay based on image processing of stained cells was proposed for microfluidic 3D culture (Ong, 2020).

#### *Commercially Available Systems*

Several commercial systems for cell viability measurement are available on the market, offering various features in terms of sensitivity, throughput and accuracy. Below are some of the most widely used systems:

- The xCELLigence Real-Time Cell Analysis (RTCA) System from ACEA Biosciences (Agilent) is based on label-free impedance measurements. It supports high-throughput applications with 96-well plates but can hardly be implemented for online measurements.
- The LUNA II (Logos Biosystems) and Vi-CELL™ XR Cell Viability Analyzer (Beckman) automate the trypan blue exclusion assay after sampling of cell suspension.
- The Fluidlab-R-300 (System C Bioprocess) rely on lens less imaging or holographic digital microscopy. It also allows optical spectral recording.
- Specific kits can be purchased for viability/cytotoxicity assessment. The LIVE/DEAD™ Viability/Cytotoxicity Kit (Thermo Fisher) allows fluorescence measurement which can be measured by cytometers, fluorescence microscope and automated plate readers.

In summary, the measurement of cell viability has evolved significantly with methods ranging from dye exclusion assays to advanced real-time label-free technologies. Traditional techniques remain widely used because of their simplicity, while new methods such as impedance-based assays or microfluidics offer improved accuracy and physiological relevance. The choice of method depends on specific experimental context, balancing cost, complexity and/or data quality. It should be noted that the discrepancy between methods is related to either predominant T-cell death process and/or type of biophysical interaction phenomena exploited for viability measurement. Most of the methods presented above require sampling, while others rely on mixing reagents with cell culture. Therefore, they are not suitable for label-free, online and/or real-time measurements.

In this paper, we propose a proof of concept for a white light spectroscopy method to assess cell quality/viability without specific reagents using lymphocyte line and inducing cell death processes. The method can be easily transferred to an online and sampling less system. The materials and methods are described in section 2, while the results are presented in section 3. A discussion is then proposed including some medico-economic considerations about CAR T-cells before concluding.

## 2 MATERIAL AND METHODS

The CEM-C1 T lymphoblast line was used in this study. Cell death was induced in two ways: X ray irradiation and storage at a temperature between 4°C and 37°C. Cell viability of both normal and dying/dead cells was then measured using an automated cell counting, flow cytometry, and white light spectroscopy. The aim is to establish a spectroscopic criterion that accounts for the loss of cell integrity, and to correlate this criterion with viabilities measured by conventional techniques.

### 2.1 Design of the Experimental Protocols

#### *X-Ray Induced Cell Death*

A total of 7 experiments were performed with both normal and irradiated cells. The experimental protocol is shown in figure 1(a).

#### *Low Temperature -Induced Cell Death*

A total of 3 experiments were performed with cells stored at 4°C, 25 °C and 37°C for each experiment. The protocol is presented in figure 1(b).

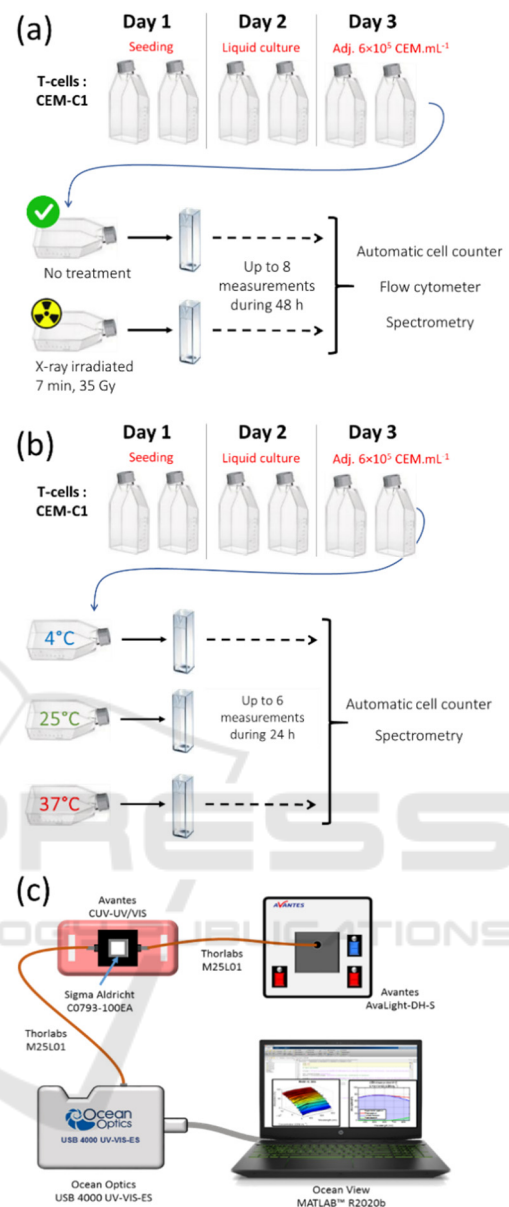


Figure 1: Design of the experimental protocols and spectra measurement setup. (a) Cell death is induced by (a) X-ray exposure ( $n = 7$ ). (b) storage at low temperature ( $n = 3$ ). (c) Absorption spectra measurement setup (from (Wacogne, 2022)).

### 2.2 Cell Culture, Death Induction and Viability Measurements

#### *Cell Culture*

The human T lymphoblast T-cell line CEM-C1 (ATCC® CRL-2265 TM) was cultured between  $5 \times 10^5$  and  $2 \times 10^6$  cells/mL in RPMI 1640 medium without Phenol Red (Gibco #11835030) and

supplemented with 10% FBS (Gibco #A5670701) and 1% penicillin/streptomycin solution (PS, Gibco #15140122) at 37 °C in a 5% CO<sub>2</sub> humidified incubator. CEM-C1 were seeding at  $6 \times 10^5$  cells/mL in RPMI 1640 medium without Phenol + 10% FBS + 1% PS.

#### *Cell Death Induction*

For X-ray death induction, suspensions were submitted to X-ray exposition for a total dose of 35Gy for 7 min. Non-irradiated and irradiated cells were then cultured at 37 °C in a 5% CO<sub>2</sub> humidified incubator and monitored during 48h.

For low temperature death induction, suspensions were simply stored at 4°C, 25°C and at 37°C. They were monitored during 24 hours.

#### *Viability and Quality Measurements*

For X-ray death induction, cell viability was assessed in three ways depending on equipment availability. (i) A LUNA-II automated cell counter (Automated Cell Counter, Logos Biosystems) was used on 5/7 experiments by mixing (V/V) cell suspensions and Trypan Blue (15250061, Fischer Scientific). (ii) Viability, apoptosis and necrosis were evaluated by cell staining using Annexin-V coupled to FITC and 7-AAD according to provider's instructions (Annexin V Apoptosis Detection Kit, BD Bioscience #556547). Viable (AnV-7AAD-), apoptotic (AnV+7AAD-) and necrotic (AnV+7AAD+) cell percentages were determined by flow cytometry (SP6800, Sony Biotechnologies). (iii) White light spectroscopy was used as detailed below and in section 2.3 on the 7 experiments.

For low temperature death induction, only automated counting and spectroscopy were used.

### **2.3 Spectra Acquisition Setup and Data Processing**

The experimental setup for spectra acquisition is simple as it only includes a white light source, a cuvette holder and a compact spectrometer (figure 1(c) issued from (Wacogne, 2022)). Spectra were acquired with 3647 data points between 177 nm and 892 nm wavelength. They were truncated to keep the range between 350 and 850 nm wavelength where the signal-to-noise ratio is higher.

Spectra were recorded in transmission and converted to absorption spectra for mathematical treatments. Trends of experimental data were calculated using the "Smoothing Spline" feature of the Matlab™ Curve Fitting toolbox with a smoothing parameter set to  $2.25 \times 10^{-3}$ .

Spurious peaks due to strong emission lines from the deuterium lamp (around 485 and 655 nm wavelength) were mathematically removed, as well as the still not fully understood additional signal at 410 nm wavelength (Wacogne, 2023). Pre-processing and subsequent data processing were performed with Matlab™ version R2020b.

For X-ray death induction, transmission spectra were recorded every 2 hours on the first day and at T=24, 30, and 48 hours thereafter. Some spectra were missing due to experimental difficulties: T0 for normal and irradiated cells exp. #4 and #5, T8 for normal and irradiated cells exp. #6. 3 normal cell spectra were not included due to too high cell concentration resulting in saturated absorption spectra: T48 exp. #2, T30 and T48 exp. 3. In total, 50 spectra were recorded with normal cells and 53 with irradiated cells. They were processed to calculate quality values (see below), which were compared with viabilities measured by either the LUNA-II automated cell counter or by cytometry.

For low temperature death induction, experiments were performed in two ways: (i) cells were prepared in the morning, stored at different temperatures and transmission spectra were recorded every 2 hours until the morning after (except during the night), (ii) cells were prepared in the evening, 1 transmission spectrum was recorded in the evening and the others the next day. A total of 72 measurements were made.

## **3 RESULTS**

### **3.1 Defining a Quality Value of Cell Suspensions**

The basic principle is based on a number of observations. (i) Healthy cells divide efficiently and few small particles (vesicles, apoptotic and necrotic bodies...) are generated, leading to high viability. Conversely, a culture with low cell viability contains a high concentration of small particles. (ii) From an optical point of view, a suspension of healthy cells contains mainly cells (large particles), light propagates mainly in a straight line, and light-matter interaction results mainly in absorption. (iii) A low-quality suspension contains a large number of small particles that scatter light. This scattering increases according to  $1/\lambda$  for micron-sized particles. From this we deduce that a high viability culture will have an absorption spectrum that reflects only the absorption of the cells, and whose shape is vaguely Gaussian, figure 2(a). Conversely, a low viability culture will

see the shape of its absorption spectrum distorted by the  $1/\lambda$  component of the scattering, figure 2(b). Thus, the higher the quality of a culture, the more Gaussian the shape of its absorption spectrum. Note that the spectra shown in figure 2 and 3 correspond to unpublished data and are used for illustrative purposes.

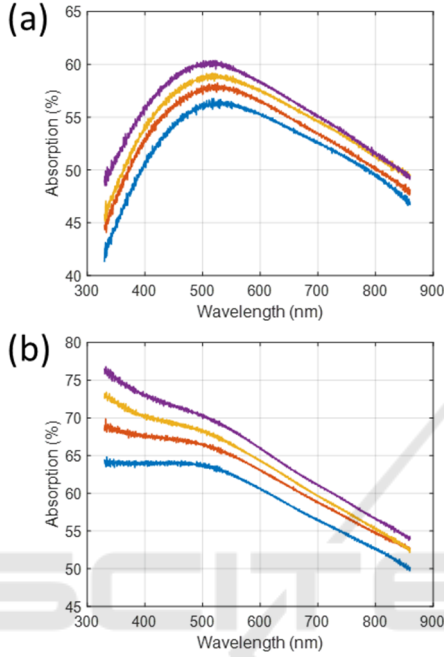


Figure 2: Examples of cell suspensions with (a) high and (b) low viability.

It must therefore be possible to estimate the viability of a suspension by the more or less Gaussian appearance of its absorption spectrum. One method is to fit the absorption spectrum with a Gaussian function. The  $R^2$  of the fit then reflects the Gaussian aspect of the spectrum and is therefore a measure of the quality of the cell suspension. A suspension quality value is defined by:  $Q=100 \cdot R^2$  expressed in %,  $R^2$  resulting from the fitting of the absorption spectrum by the following function:

$$abs(\lambda) = a \cdot \exp\left(-\left(\frac{\lambda - b}{c}\right)^2\right) + d \quad (1)$$

In equation (1),  $abs(\lambda)$  is the absorption spectrum, a, b, c and d are the fitted coefficients.

Figure 3 shows examples of fitting obtained using equation (1) on both types of suspensions.

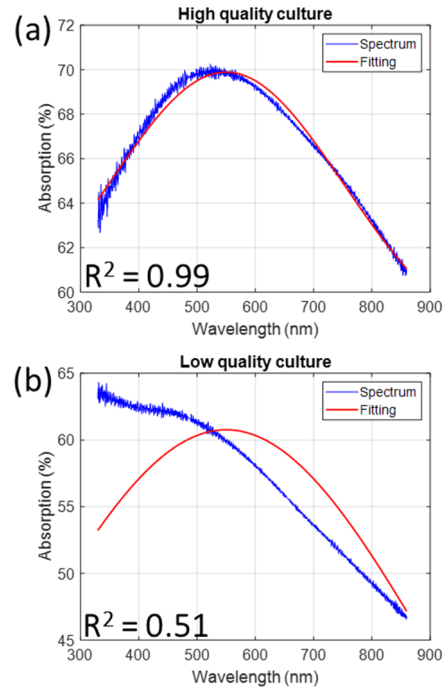


Figure 3: Examples of Gaussian fitting with (a) high and (b) low viability.

However, a few precautions need to be taken. If no constraints are imposed on the fitting coefficients, the algorithm always manages to find a quadruplet leading to a high  $R^2$ . The constraints imposed on the coefficients in this work are shown in Table 1.

Table 1: Variation intervals of fitting coefficients.

| Coeff.    | a (%) | b (nm) | c (nm) | d (%) |
|-----------|-------|--------|--------|-------|
| Low. lim. | 0     | 550    | 0      | 0     |
| Upp. Lim. | 200   | 700    | 500    | 200   |

### 3.2 Comparison of Viability and Quality of Non-Irradiated and Irradiated Cells

Figure 4 shows examples of spectra recorded with non-irradiated and irradiated cells. For non-irradiated cells, the concentration increased from  $6 \times 10^5$  to  $13 \times 10^5$  cell.mL<sup>-1</sup> during the 48-hours experiment. The generation time was 44 hours, which was longer than that measured in previous experiments due to slight differences in the culture protocol. Concentrations were measured by the method described earlier (Wacogne, 2022). For irradiated cells, the concentration decreased from  $6 \times 10^5$  to  $2 \times 10^5$  cell.mL<sup>-1</sup>, which was expected. In this case, the concentration was measured spectrally using a more advanced method than the one used in 2022.

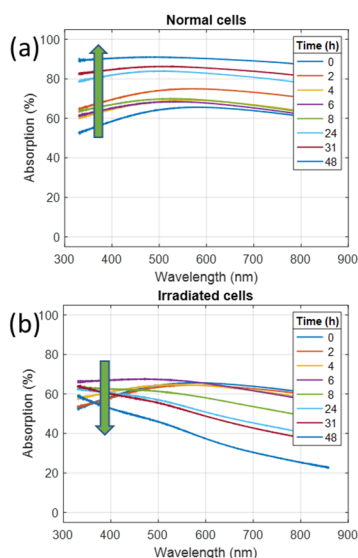


Figure 4: Examples of spectra recorded with (a) non-irradiated cells and (b) irradiated cells. Green arrows show either increasing or decreasing concentration.

Figure 5 shows quality values calculated from absorption spectra and viabilities measured with the automated counter and the cytometer, along with the corresponding trends corresponding to the data shown in figure 4.

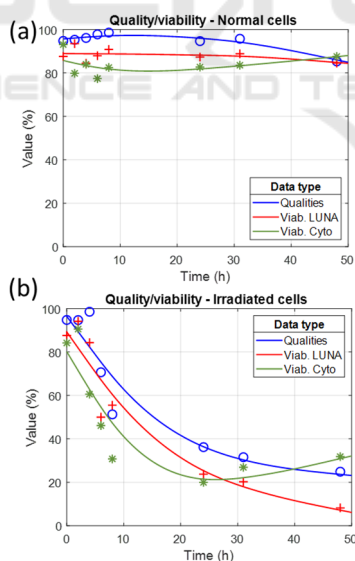


Figure 5: Quality values and viabilities corresponding to spectra of figure 4 for (a) non-irradiated cells and (b) irradiated cells. Markers: experimental data. Lines: trends.

A correlation was observed between qualities measured with white light spectroscopy and conventionally measured viability. Trends show an unexpected increase in viability as measured by

cytometry at the end of the experiment. This was often observed and will be addressed in section 4.

Experimental data show dispersion around corresponding trends. Dispersion was calculated using a modified form of the standard deviation calculation where the mean is replaced by the trend as follows.

$$Disp = \sqrt{\frac{1}{n} \sum_{i=1}^n (Value_i - Trend_i)^2} \quad (2)$$

In equation (2),  $Value_i$  represents the  $i^{th}$  data point and  $Trend_i$  is the value of the corresponding trend at data  $i$ .

Dispersion was then calculated for each measurement method for both non-irradiated and irradiated cells (figure 6).

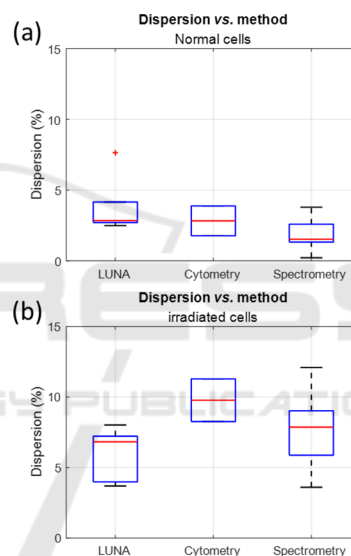


Figure 6: Boxplot of dispersion for the different measurement methods for (a) non-irradiated and (b) irradiated cells.

Dispersion was quite low for non-irradiated cells (median less than 3%), while it was significantly higher for irradiated cells (median over 6.5%). Spectral measurements showed the lowest dispersion for non-irradiated cells, while automated counting was the best option for measuring the viability of irradiated cells. Dispersion of viability measured by cytometry was quite large with a median value close to 10%. Considerations about dispersions will be discussed in section 4.

The correlation between quality values and viability, as measured by either the automated counter or the cytometer was reported (figure 7). To avoid cluttering the figure in the (100,100) coordinate

region, only data corresponding to irradiated cells were showed in this figure.

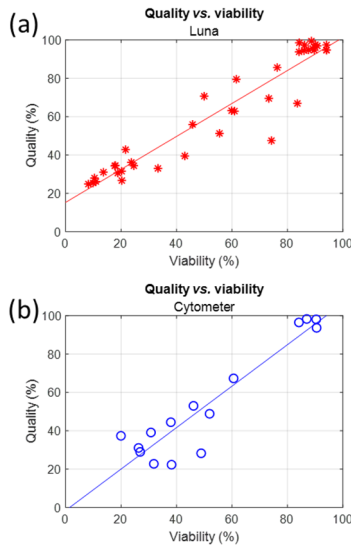


Figure 7: Relation between quality and viability for (a) automated counting and (b) cytometry.

Because of the dispersion shown in figure 6, the data shown in figure 7 also showed a large dispersion. The dispersion was 8.6% for the (quality/counter) results and 10% for the (quality/cytometer) results. This aspect will be discussed in section 4. Nevertheless, linear regressions could be calculated with acceptable  $R^2$  around 0.9. The linear regressions for both cases are given below.

$$Quality = 0.86 \times Viab_{Counter} + 15.3 \quad (3)$$

$$Quality = 1.08 \times Viab_{Cytometer} - 1.55 \quad (4)$$

The difference between these regressions will be discussed in section 4.

### 3.3 Comparison of Viability and Quality of Cells Stored at Low Temperature

Figure 8 shows examples of spectra recorded at different temperatures. At 37°C, the concentration normally increases from  $5.6 \times 10^5$  to  $7.6 \times 10^5$  cell.mL<sup>-1</sup> in 24 hours (generation time: 35 hours). The shape of the spectra remains constant over time. At 25°C, the concentration decreases slightly from  $5.5 \times 10^5$  to  $5.1 \times 10^5$  cell.mL<sup>-1</sup> and the shape of the spectra starts changing after 21 hours. At 4°C, the concentration decreases sharply from  $5.5 \times 10^5$  to  $3.6 \times 10^5$  cell.mL<sup>-1</sup> while the shape of the spectra changes much earlier.

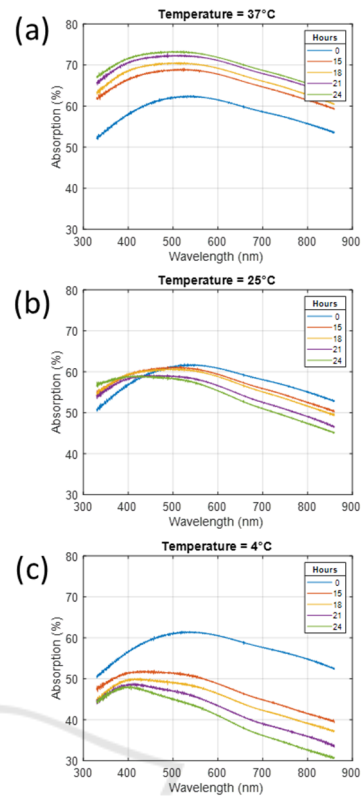


Figure 8: Examples of spectra recorded at (a) 37°C, (b) 25°C and (c) 4°C.

Figure 9 shows the evolution of the corresponding viability and quality. The evolution of these values is consistent with the spectra shown in figure 8.

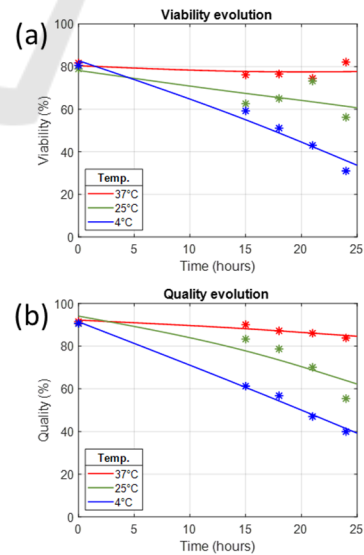


Figure 9: Viability and quality evolution corresponding to spectra shown in figure 7. (a) Viability measured with automated counter, (b) Quality.

Finally, figure 10 shows the linear correlation between viability and quality for all data recorded at 25°C and 4°C (37°C was omitted to avoid cluttering the figure in the (100,100) coordinate region).

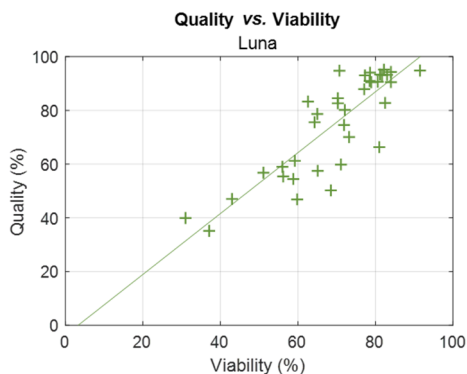


Figure 10: Relation between viability (counter) and quality (spectroscopy).

The data dispersion is high for the reasons mentioned above. The linear regression is shown below.

$$Quality = 1.13 \times Viab_{counter} - 3.75 \quad (5)$$

In conclusion, according to the results shown in the above sections, a relationship exists between quality measured spectrally and viability measured by either conventional methods. This relationship is linear and depends on both the conventional method used as a gold standard and the death process the cells undergo. White light spectroscopy can therefore be used to measure the viability of a cell suspension but should apparently be adapted to experimental conditions. However, the quality value may also be an alternative method to estimate the cell health as discussed in section 4.

## 4 DISCUSSION

### Data Format

The original experimental setup was used to measure cell concentrations. A discussion of data format was proposed to explain why spectra were presented in terms of absorbance rather than other formats such as transmission or optical densities (OD) (Wacogne, 2022). In the current work, spectra were recorded in the same way to facilitate mathematical treatments. Note that the word "absorption" can sometimes be a misnomer when considering small size particles, as discussed later on.

### Temperature-Induced Death Data

Experiments were performed in two ways: (i) cells were prepared in the morning, stored at different temperatures and transmission spectra were recorded every 2 hours until the next morning, (ii) cells were prepared in the evening, one transmission spectrum was recorded in the evening and the others the next day. Since viability decreases quite slowly when cell death is induced by temperature stress, nothing happens on the first day if the experiment was started in the morning. Therefore, the examples shown in figures 8 and 9 correspond to experiments started in the evening.

### Light-Matter Interaction, Spectra Shapes and Remarks Concerning Optical Densities

The light-matter interaction process depends on the size of the illuminated particles (figure 11).

|   | What is not detected   | Typical spectra |
|---|--|-----------------|
| <b>Big particles (T-cells)</b><br><b>10 μm</b><br>Mostly straight propagation                                 | <ul style="list-style-type: none"> <li>• Large cell absorption</li> <li>• Little diffusion</li> </ul>                                      |                 |
| <b>Small particles (big vesicles, apoptotic bodies...)</b><br><b>0.5-1.5 μm</b><br>Propagation with diffusion | <ul style="list-style-type: none"> <li>• Little absorption</li> <li>• Large diffusion</li> <li>• 1/λ behaviour</li> </ul>                  |                 |
| <b>Very small particles (vesicles)</b><br><b>150 nm</b><br>Mostly diffusion                                   | <ul style="list-style-type: none"> <li>• Very little absorption</li> <li>• Large diffusion</li> <li>• 1/λ<sup>4</sup> behaviour</li> </ul> |                 |
| <b>Proteins, molecules</b><br><b>3-10 nm</b><br>Straight-line propagation                                     | <ul style="list-style-type: none"> <li>• Molar absorptivity</li> <li>• Homogeneous medium</li> </ul>                                       |                 |

Figure 11: Light-matter interaction with particles.

When the particles are large (around 10μm), the light propagates mostly straight and there is very little diffusion. In this case, the dominant light-matter interaction process is absorption by cell constituents. Spectrally, the shape of the absorption spectrum is approximately Gaussian, at least for T-cells (figure 2(a)).

For smaller particles (around 1 μm), there is little absorption and diffusion predominates. In this case, diffusion evolves according to 1/λ, which explains the spectra shape when large and small particles are present (figure 2(b)).

For even smaller particles, diffusion is clearly dominant and evolves according to 1/λ<sup>4</sup>.

Finally, for molecular size events, the medium can be considered homogeneous and only absorption occurs according to the molar absorptivity of the molecules.

In this work, cell suspensions with high viability correspond to the first row of figure 11, while



suspensions with low viability (regardless of the death induction method) correspond to the second row of figure 11. It is therefore inappropriate to speak of absorption when the dominant light-matter interaction is diffusion. In fact, the light not incident on the spectrometer has not only been absorbed, but mainly diffused. In this case, the word attenuation may be preferred (Wacogne, 2023).

Also, the term optical density theoretically refers only to the absorption of homogeneous media (fourth row in figure 11). In other situations, such as measuring the concentration of a bacterial suspension using a plate reader, the term optical density is inappropriate. Nevertheless, the Beer-Lambert law can still be applied (especially the law of OD additivity for reference taking), but a term other than OD should be preferred.

#### *Data Dispersion*

Dispersion is clearly observed in viability and quality measurements. Dispersion can have several causes, as already mentioned (Wacogne, 2022, 2023) for cell concentration measurements. With conventional techniques, viability measurements are performed with very small volumes (a few tens of  $\mu\text{L}$ ), making the measurement poorly representative of what is actually present in the culture cuvettes. The low-cost plastic cuvettes used in this work have variations in their optical properties that lead to inaccuracies of a few percent.

The results presented here suggest that the dispersion was even greater when viability was measured. This is probably due to the difficulty for conventional systems to actually determine whether a cell is alive or dead. This results in a large dispersion of data when the relationship between quality and viability measured by either conventional mean is reported (figures 7 and 10). This dispersion is not due to possible inaccuracies in the measurement of quality by spectroscopy since optical spectroscopy proved to be more accurate than automated counter for cell concentration measurements (Wacogne, 2021). We could have then thought that quality measurements would have shown less dispersion than other conventional means. It is not the case. One hypothesis is that equation (1) used to fit spectra could be improved and/or that fitting intervals reported in table 1 could be adjusted. Indeed, the equation describing the shape of the absorption spectra of CEM-C1 cells includes a wavelength dependent base line not accounted for in equation (1) (equation (5); Wacogne, 2022).

#### *Relationships Between Quality and Viability*

Figure 7 shows the relationships between quality and viability when cell death is induced by irradiation for 2 gold standard techniques: automated counting and cytometry. The relationships differ in terms of linear regression slopes and ordinates at the origin. Figure 10 shows the relationship between viability, as measured by automated counting, and quality when cell death is thermally induced. It differs from the counting/spectroscopy (irradiation) relationship, but is similar to the cytometry/spectroscopy (irradiation) relationship.

Viability measurement depends on several factors. The discrepancy between methods is related to either the predominant T-cell death process and/or the type of biophysical interaction phenomena used for viability measurement (Chung, 2015, Fotakis, 2006 and Chan, 2015). In fact, it depends on the type of cell death and the ability of the viability measurement equipment to detect it.

When cells die, they can undergo either apoptosis or necrosis (autophagy is not discussed here). In its early stages, apoptosis is characterised by a slight reduction in cell size (a few  $\mu\text{m}$ ). Later, the cells disappear, producing micro- and sub-micrometre-sized apoptotic bodies and microvesicles. In its early stages, necrosis is characterised by a slight swelling of cells. Later, cell membranes rupture and release micro- and sub-micrometre-sized necrotic bodies. Cell membrane debris remains in the suspension.

In this paper, viability is measured by cytometry or automatic counting. The cytometric markers used in this study makes it possible to distinguish apoptosis from necrosis. Every not marked and cell-sized event is considered as a living cell. The automatic counter is based on trypan blue staining. This dye penetrates cells but is expelled by living cells. It therefore stains cells undergoing early necrosis. Early apoptotic and late and large necrotic bodies are either stained or not depending on individual death state. Late apoptotic and small necrotic bodies are not detected.

The quality measured spectrally reflects the extent to which the shape of the measured spectrum deviates from a Gaussian shape. A decrease in this quality value therefore reflects the presence of particles smaller than healthy cells in the suspension, whatever the type of cell death. It is mostly late apoptotic and necrotic bodies, including cell membrane debris, that modify the shape of the measured spectrum.

Regarding X ray induced cell death and to understand the differences between the relationships shown in figure 7, it is important to distinguish between the ability of conventional viability

measurement methods to actually produce accurate results when viability is either high or low.

*High viability range.* The automated counter, based on trypan blue staining, easily detects early necrotic cells and hardly detects late necrotic bodies. Some early apoptotic cells are detected while no late apoptotic bodies are seen. This leads to an overestimation of viability by automated counting when viability is high, already reported previously (Cai, 2023). To account for this, the data shown in figure 7(a) should be slightly shifted to the left in the high viability range, thus increasing the slope of the relationship and decreasing the ordinate at the origin.

*Low viability range.* In this case, cytometry barely detects dead cells. In fact, cells at this stage of death are weakly expressing targets for AnV and 7AAD markers, and both late apoptotic and necrotic bodies are barely detectable. This leads to an overestimation of viability by cytometry when viability is low. Indeed, this is the reason why the apparent viability increased between 24 and 48 hours post-irradiation (figure 5(b)). To account for this, the data shown in figure 7(b) should be shifted slightly to the left in the low viability range, thus decreasing the slope of the relationship and increasing the ordinate at the origin.

Taking all these corrections into account should reduce and perhaps eliminate the differences in the relationships shown in Figure 7 and equations (3) and (4).

With regard to the effect of temperature, it is difficult to interpret the relationship shown in figure 10 and equation (5) without comparison with other measurement methods. The fact that the slope is equal to 1 and the ordinate at the origin is equal to 0 does not lead to any conclusion at this stage. It is not possible to estimate the predominant T-cell death process occurring at low temperature from these data. However, it was reported that hypothermia mainly induces apoptosis (Rauen, 1999; Wang, 2017).

#### *Quality as a More General Alternative to Viability?*

The measurement of viability remains open to question since it depends on type of cell death and of biophysical interaction phenomenon used in the different measurement techniques. This explains the differences observed in the literature when different techniques are compared.

Apart from specific applications where the cell death process is being studied, viability measurements are mainly used to assess the health of cell cultures, to evaluate experimental effects or to optimise culture conditions. High cell viability indicates a healthy and robust culture, whereas low viability indicates problems with the culture

conditions or possible contamination. In these cases, the spectrally measured quality value could provide a more general alternative to viability measurement. Indeed, the quality value indicates the extent to which the cell suspension deviates from an ideal situation where all cells are viable without relying to any bio-physical-chemical interactions or equipment specificity. Noted that early apoptotic and necrotic bodies do not alter the spectra shape as much as late bodies. An adjustment of equation (1) and/or table (1) may be necessary to account for these slight spectral changes.

#### *Medico-Economic Considerations about CAR T-Cells*

This study may have applications into the field of CAR T-cell production and in particular the expansion phase of several days, with each additional day increasing their cost. Quality controls are currently used to follow cell expansion but requires frequent sampling, increasing risk of contamination. The results outlined above are particularly noteworthy because they enable quality control without the need for sampling and allow for a rapid termination of the expansion phase if issues arise.

CAR T therapy, designed to treat patients with currently incurable diseases, has the potential to revolutionize treatment in the coming years. However, it remains still challenging to predict the range of diseases these therapies may address or how many patients might ultimately benefit from them.

Currently, there are several CAR T therapies on the market (Wang, 2023; Bogert, 2021), each with high price tags due to the complexity of treatment and production. Some of the prominent FDA-approved CAR T therapies include:

- Kymriah (tisagenlecleucel): Used to treat acute lymphoblastic leukemia (ALL) and certain types of lymphoma. It costs approximately \$475,000 per dose.
- Yescarta (axicabtagene ciloleucel): Primarily used for large B-cell lymphoma, with a cost of around \$373,000 per dose.
- Tecartus (brexucabtagene autoleucel): Approved for mantle cell lymphoma, priced similarly to Yescarta at around \$373,000.
- Breyanzi (lisocabtagene maraleucel): Treats large B-cell lymphoma and has a list price of about \$410,000 per dose.
- Abecma (idecabtagene vicleucel): Approved for multiple myeloma, costing around \$419,500 per dose.

These therapies, while promising in treating various blood cancers, also incur additional costs

related to hospitalization and managing side effects like cytokine release syndrome (CRS). This often pushes the total cost per patient toward or beyond \$1 million (Bogert, 2021; The ASCOP Post, 2018).

Automating CAR-T-cell production could significantly reduce costs by lowering the need for specialized labour and minimizing errors, thus addressing the high price of treatments. It would also improve scalability, enabling faster production and wider accessibility. Standardizing the process could enhance consistency, leading to better therapeutic outcomes. Automation would also shorten the turnaround time, allowing patients to start treatment sooner, reducing need for costly interim therapies. Finally, automating production could lower healthcare burdens and make CAR T more accessible.

#### *Online Integration Possibilities*

White light spectroscopy can be easily integrated into an online system (Wacogne, 2020). This is directly in line with the advantages of automating the manufacture of CAR T mentioned above. In addition, the use of extremely compact light sources (Yujileds) and spectrometers of fingernail size (Hamamatsu) should facilitate and accelerate the integration of this method.

Thus, having an online, real-time system for monitoring cell expansion, quality of cells produced and, potentially, real-time detection of any contamination would represent a definite added value for the development of these production systems.

## 5 CONCLUSIONS

In this paper, white light spectroscopy is used to estimate the viability of T-cell line suspensions using a “quality value” determined from the shape of the absorption spectra of cell suspensions. A direct relationship is observed between this quality value and the viability measured by various conventional methods. However, this relationship depends on the conventional system used and the way in which cell death is induced. These discrepancies in viability measurements has already been mentioned in the literature when comparing different conventional methods.

Measuring the “quality value” could provide an alternative to viability assessment less dependent on equipment and type of cell death involved because it is based solely on analysis of spectra shape and independent from complex biophysical-chemical interactions.

The measurement of a single absorption spectrum of lymphocyte suspensions makes it possible to monitor cell concentration and possibly detect any contamination, but also to assess quality/viability of cell cultures during the production of CAR T therapies, leading to the possible online integration of white light interferometry. This possibility of automation would then be a step towards reducing the price of these innovative therapies and making their use more democratic.

## ACKNOWLEDGEMENTS

This work was supported by the MiMedI project (Grant N° DOS0060162/00) and the BioIMP project (Grant N° BFC000802) funded by EU through the European Regional Development Fund of the Region Bourgogne Franche-Comté.

## REFERENCES

- Agilent: [https://www.agilent.com/en/product/cell-analysis/real-time-cell-analysis/rtca-analyzers/xcelligence-rtca-esight-imaging-impedance-741228?gad\\_source=1&gclid=Cj0KCQjw3vO3BhCqARIsAEWblcCSop2Rma9nWV2mnlpm1rzBEmhuFsxR3WFYtNWWCzbMyZ6vGHjDzBcaAtSMEALw\\_wcB&gclidsrc=aw.ds](https://www.agilent.com/en/product/cell-analysis/real-time-cell-analysis/rtca-analyzers/xcelligence-rtca-esight-imaging-impedance-741228?gad_source=1&gclid=Cj0KCQjw3vO3BhCqARIsAEWblcCSop2Rma9nWV2mnlpm1rzBEmhuFsxR3WFYtNWWCzbMyZ6vGHjDzBcaAtSMEALw_wcB&gclidsrc=aw.ds)
- Beckman: <https://www.beckman.fr/cell-counters-and-analyzers/vi-cell-xr>
- Berridge, M. V., et al, 2016. Tetrazolium dyes as tools in cell biology: New insights into their cellular reduction. *Biotechnology Annual Review*, Vol. 11, pp.127-152
- Bogert, R. 2021. Improving Outcomes and Mitigating Costs Associated With CAR T-Cell Therapy. *Supplement to the American Journal of Managed Care*, Vol. 27, pp. S253-S261
- Cai, Y., et al, 2024. Assessment and comparison of viability assays for cellular products, *Cytotherapy*, Vol. 26, pp. 201-209
- Chan, L.L., et al, 2015. Morphological observation and analysis using automated image cytometry for the comparison of trypan blue and fluorescence-based viability detection method, *Cytotechnology*, Vol. 67, pp. 461-473
- Chung, D.M., et al, 2015. Evaluation of MTT and Trypan Blue assays for radiation-induced cell viability test in HepG2 cells. *Int J Radiat Res*, Vol. 13, pp. 331-335
- Fotakis, G., et al, 2006. In vitro cytotoxicity assays: Comparison of LDH, neutral red, MTT and protein assay in hepatoma cell lines following exposure to cadmium chloride, *Toxicology Letters*, Vol. 160, pp. 171-177
- Fuente-Jiménez, J.L., et al, 2023. A comparative and Critical Analysis for In Vitro Cytotoxic Evaluation of Magneto-Crystalline Zinc Ferrite Nanoparticles Using

- MTT, Crystal Violet, LDH, and Apoptosis Assay. *Int. J. of Mol. Sci.*, Vol. 24, PP. 12860
- Hamalainen-Laanaya, H.K., et al, 2012. Analysis of cell viability using time-dependent increase in fluorescence intensity. *Analytical Biochemistry*, Vol. 429, pp. 32-38
- Hamamatsu: <https://www.hamamatsu.com/eu/en/product/optical-sensors/spectrometers/mini-spectrometer.html>
- Kumar, G., et al, 2015. Flow cytometry evaluation of in vitro cellular necrosis and apoptosis induced by silver nanoparticles, *Food and Chemical Toxicity*, Vol. 85, pp. 45-51
- Logos Biosystems: <https://logosbio.com/>
- Louis, K.S., et al. 2011. Cell Viability Analysis Using Trypan Blue: Manual and Automated Methods. Stoddart, M. (eds) *Mammalian Cell Viability. Methods in Molecular Biology*, Vol. 740, pp. 7-12
- Macklin, C.C., et al, 1920. A study of brain repair in the rat by the use of trypan blue: with special reference to the vital staining of the macrophages. *Archives of Neurology and psychiatry*, Vol. 7, pp. 353-NP
- Ong, L.J.Y., et al, 2020. Quantitative Image-Based Cell Viability (QuantICV) Assay for Microfluidic 3D Tissue Culture Applications. *Micromachines*, Vol.11, pp. 669
- Optiz, C., et al, 2019. Rapid determination of general cell status, cell viability, and optimal harvest time in eukaryotic cell cultures by impedance flow cytometry. *Applied Microbiology and Biotechnology*, Vol. 103, pp. 8619-8629
- Rauen, U., et al, 1999. Cold-induced apoptosis in cultured hepatocytes and liver endothelial cells: mediation by reactive oxygen species. *Faseb journal*, Vol. 13, pp.155-168
- Sarma, K.D., et al, 2000. Improved sensitivity of trypan blue dye exclusion assay with Ni<sup>2+</sup> or Co<sup>2+</sup> salts. *Cytotechnology*, Vol. 32, pp. 93-95
- Schneckenburger, H., et al, 2012. Light exposure and cell viability in fluorescence microscopy. *Journal of Microscopy*, Vol. 245, pp. 311-318
- Shenkin, M., et al, 2007. Accurate assessment of cell count and viability with a flow cytometer. *Cytometry Part B: Clinical Cytometry*, Vol.72B, pp. 427-432
- Stoddart, M. J. 2011. Cell Viability Assays: Introduction. *Methods in Molecular Biology*, Vol. 740, pp. 1-6
- System C Bioprocess: <https://www.system-c-bioprocess.com/produit/fluidlab-r-300/>
- The ASCO Post: <https://ascopost.com/issues/may-25-2018/weighing-the-cost-and-value-of-car-t-cell-therapy/>
- Thermofisher: <https://www.thermofisher.com/order/catalog/product/L3224>
- Tsaouis, K., et al, 2013. Time-dependent morphological alterations and viability of cultured human trabecular cells after exposure to Trypan blue. *Clinical & Experimental Ophthalmology*, Vol. 41, pp. 484-490
- Wacogne, B.; et al, 2020, Optical Spectroscopy for the Quality Control of ATMP fabrication: A new method to monitor cell expansion and to detect contaminations, In *Proceedings of the 13th International Joint Conference on Biomedical Engineering Systems and Technologies (BIOSTEC 2020)*, Springer Vol. 1, pp. 64-72
- Wacogne, B. et al, 2021. White light spectroscopy for T-cell culture growth monitoring: towards a real-time and sampling free device for ATMPs production. *Journal of Translational Science*, Vol. 7, pp. 1-10
- Wacogne, B., et al, 2022. Absorption Spectra Description for T-Cell Concentrations Determination and Simultaneous Measurements of Species during Co-Cultures, *Sensors*, Vol. 22, art. 9223
- Wacogne, B., et al, 2023. Absorption/attenuation spectra description of ESKAPEE bacteria: application to seeder-free culture monitoring, mammalian T-cell and bacteria mixture analysis and contamination description, *Sensors*, Vol. 23, art. 4325
- Wang, J., et al, 2017. The analysis of viability for mammalian cells treated at different temperatures and its application in cell shipment. *PLoS ONE* 12, Vol.4, pp. e0176120
- Wang J.Y., et al, 2023. CAR-T-cell therapy: Where are we now, and where are we heading?, *Blood Sci.*, Vol. 5, pp. 237-248.
- Wang, X., et al, 2016. Clinical manufacturing of CAR T-cells: Foundation of a promising therapy, *Mol. Ther. Oncolytics*, Vol. 3, pp. 16015
- Yang, B., et al, 2023. Label-Free Sensing of Cell Viability Using a Low-Cost Impedance Cytometry Device. *Micromachines*, Vol. 14, pp. 407
- YUJILEDs : <https://store.yujiintl.com/products/yujileds-hyperspectral-350nm-1000nm-0-4w-led-smd-2835>
- Zhong, J., et al, 2021. Multi-frequency single cell electrical impedance measurement for label-free cell viability analysis. *Analyst*, Vol. 146, pp. 1848-1858
- Zou, Y., et al. 2013. Application of LDH-Release Assay to Cellular-Level Evaluation of the Toxic Potential of Harmful Algal Species, *Bioscience, Biotechnology, and Biochemistry*, Vol. 77, pp. 345-352